
2019 Washington University in St. Louis Design Report

The WUFR-19 was designed around the twin premises of drivability and adjustability. Throughout the design process, we focused on improving controllability, adjustability, and predictability. Focusing on these criteria translates into an increased ability to push the limits of the car's handling, acceleration and braking. It will mean the difference between hitting every corner's apex and falling off the racing line, between launching the car properly every time and spinning the wheels, and between consistently posting quick lap times and falling behind.

Suspension

Suspension design began with the analysis of tire data and collected sensor data so we could fully understand the maximum tractive capabilities and ideal operating ranges of different parameters and components. Using this analysis, our wheels and tires were selected to optimize unsprung mass and grip. These wheels were selected to reduce corner weight despite the increase in reaction loads in linkages by decreasing spacing. Our tires were chosen after an analysis of the desired tractive response of the car with the Pacejka Magic Formula 6.1. Additionally, the suspension geometry was designed using collected accelerometer, linear potentiometer, and gyroscopic data to decrease roll center migration, optimize camber gain through the range of vehicle travel, and provide the most intuitive response. Most notably, the platform was designed for a non-aero car by prioritizing roll camber gain as opposed to heave camber and by aiming for neutral camber on our unladen tire during steer. The goal of the geometry was to achieve the largest tire contact patch possible during maximally loaded transient cases. These priorities were carried through the design of all subassemblies where physical displacements of components were restricted by the limits of performance. Specifically, while it is impossible to eradicate compliance in a system, all subassemblies were designed using a series-spring analysis of how deflection would alter performance and feedback to the driver.

Linkages

We selected high modulus carbon tubes bonded to aluminum after considering several parameters, including strength, stiffness, cost, accessibility, and repeatability of manufacturing. The tubes we selected were the best compromise, featuring much higher yield strength, less axial deflection during use, better stability in Eulerian buckling, and lower weight than our steel alternatives. Adhesive bonding preparation, bond gap, and overall reliability were tested on a universal tester so that, with a low standard deviation and within a 95% confidence interval, our final bonds are stronger than both our maximum load and the rod ends used in our system.

Rockers

We used vertical acceleration data collected from testing along with force ratios and moment balances through the system to calculate our maximum loads. The rocker structures were designed by first calculating the forces in each member at maximum load using the method of joints, then modeling the rockers in CAD with help from topology optimization software. We used FEA software to predict displacement and stress and to check against buckling and yielding. Stiffness was constrained to ensure that displacement did not alter the performance or response of the actuation system. The geometries of the rockers were designed to achieve a linear motion ratio to maintain a consistent wheel rate close to the spring rate. This helps to make the handling intuitive and reliable and to increase driver confidence through the entire range of damper-travel.

Anti-Roll

Using collected chassis torsional stiffness and accelerometer roll data, titanium rotary-blade anti-roll systems were implemented to increase lateral grip and adjustability. These data advised us on the maximum load the systems must withstand without failing based on peak values from track testing and the general operating roll range of the vehicle during autocross runs. Actuating bars with varied moments of inertia allow for systematic changes in suspension stiffness compared to a traditional drop link system. Through this analysis, subjective driver feedback can be translated to numeric adjustment by varying engagement angle. The compact assembly and the rapid adjustability of this system made it a superior choice to a conventional sway-bar style system despite the risk of increased compliance due to alignment on the car. Stiffness values and predicted response were adjusted based on theoretical losses due to absorbed compliant load.

Steering

We designed steering with a focus on achieving the smallest turn radius needed for the competition and maximizing the car's feedback to the driver by minimizing steering system compliance. For the outboard geometry, we used the relationship between slip angle, tire inclination, cornering stiffness, and lateral force data to find the maximum available steer angles for



our tires. We then consulted drivers on their ability to follow the perfect drive line around the sharpest possible corner. We used this feedback to find the target turn radius, then used this turn radius in combination with the available steer angles and our car's weight transfer throughout a turn to determine our desired wheel turn angles and the resultant ackermann. For the inboard system, we chose a steering rack that minimizes compliance throughout the assembly and a universal joint at both the upper column support and the steering rack. To justify this, we modeled a single universal joint in code, then used that code as verification for adding a second u-joint to cancel out the effect of a non-constant output velocity at extreme u-joint angles. To fully define the outboard geometry, we modeled three static systems, one at neutral steer and one at each maximum steer, to iterate through tie rod and steering arm geometries in 3D until we achieved the desired wheel turn angles.

Chassis

The chassis design was centered around developing a torsional stiffness MatLab calculator, automating geometry and thickness iterations within that simulation, lowering the engine by 1", and minimizing compliance at key nodes. Keeping with the overall design goal of adjustability, the focus on torsional stiffness was to allow for a predictable response to suspension adjustments and for sufficient variation of load transfer bias for a given suspension roll stiffness.

MatLab Torsional Stiffness Simulation

One major goal of this design cycle was to create a simulation that could accurately predict torsional stiffness and also be utilized for analysis of loads at suspension pick-up points. We adapted "MatLab Structural Analyser", which utilizes the direct stiffness method, for an FSAE frame and then implemented a genetic algorithm to optimize both geometry and thickness. The mathematical validity of this implementation was confirmed by running an equivalent simulation in Patran, which yielded a torsional stiffness prediction that was 0.24% different from the MATLAB simulation tool for the same constraints. The algorithm was given an initial rules compliant frame and then alternated between generations of geometry changes and thickness changes sorting by the ratio of torsional stiffness and weight. The results of this simulation indicated that stiffer side sections that were resistant to bending as well as higher spacing between the side sections were more effective at maximizing torsional stiffness than increased cross-bracing.

A target weight and torsional stiffness was partially found by using the peak of the torsional stiffness to weight ratio for a given geometry to gauge when diminishing returns set in for thickness changes. Then, in order to maximize the effectiveness of limited man-hours, a focus was put on maximizing the stiffness of a target weight rather than a optimizing weight for a target stiffness.

The constraints and loads of the model were validated using a test rig and a frame from a past design, which was physically tested in various states (engine in, engine out, tubes removed). This was also used to validate our model of the engine. The results of the tests showed that the discrepancy between predicted and actual torsional stiffness values could be accounted for by a constant factor.

Suspension Node Analysis

Critical suspension nodes, such as the nodes that the dampers and rockers attach to, were analyzed with the MatLab direct stiffness solver under max-loading conditions. These nodes were designed to deflect less than 0.015" so as not to introduce unpredictable levels of compliance into the suspension.

Engine Lowering & Rear Structure

Utilizing the custom oil pan, the engine was lowered by 1" decreasing the center of gravity and improving the handling characteristics of the car. This change also shortened the lengths of engine mount tubes which allowed for the engine to be better leveraged as a frame stiffener. In order to ensure easy servicing and allow for more complex upper rear geometry, the engine is inserted and removed by from underneath the frame.

Aerodynamics and Body

Accessibility-

The design of the composite parts for the WUFR-19 focused on vehicle serviceability to the cockpit along with several powertrain components. Our quarter turn fasteners reduce both fastener and tab weight for the system and increased the ease of assembly and removal. The design of the body panel extending from the front roll hoop to the bulkhead allows it to be removed using two quarter turns for easy access to the steering rack and pedal box to make adjustments for drivers. Additionally, quarter turns were also used to fasten the side pods and provide easy access to both the radiator and exhaust systems.



Aerodynamics-

A simplified solid body car model was created to gather vehicle drag data. The sidepods were designed to create an even pressure distribution across the radiator core and improve the mass flow rate through the core. Parametric CFD simulations were run on the radiator core in order to calculate the side pod inlet size relative to the radiator core dimensions. A manual code was created to compute simulation inputs, such as turbulent length scale and turbulent intensity as well as thermal and pressure boundary conditions for a range side pod inlet sizes. These simulations were based on the required engine heat rejection rate and corresponding required mass flow rate through the radiator core for sufficient heat transfer. The outlet was then sized such that the velocity exiting the side pods is equal to the free stream velocity in order to reduce drag caused by vortices.

Powertrain

The powertrain design process began this year with the selection of the engine and an overall team goal to increase drivability by creating a linear power curve and a flat torque curve. A four cylinder engine was chosen to allow for better throttle response. Hand calculations and CFD analysis of the restrictor lead to our decision to run a naturally aspirated engine, as the choked flow condition at the restrictor limited mass flow, negating some of the benefits of forced induction. 93 octane fuel was chosen over E85 because the higher energy density and stoichiometric ratio allows for better packaging and reduced fuel weight.

Exhaust-

The exhaust system was designed to have equal length long tube headers, with a 4-1 collector design geometry, ultimately cutting weight from other designs as its lighter and more compact. The exhaust header dimensions were designed by the use of theoretical equations, and with the use of matlab script theoretical exhaust header length, and pipe diameter were determined. With the use of an engine modeling software, these values were utilized and adjusted to commercial sizes to produce optimal engine performance with an increase in the exit velocity of exhaust gases and the exhaust scavenging. Our pipe diameter was chosen to improve scavenging and decrease back pressure in the system. The exhaust system was mounted in the side pod of the vehicle to improve lateral weight distribution in conjunction with the radiator.

Intake-

The engine's intake manifold was designed to compliment the exhaust manifold tuning in order to smooth out the engine's powerband to make it more predictable and driveable. The intake runner cross-sectional area was chosen to maximize air flow at high RPMs and match the engine's port geometry in order to minimize the discharge coefficient and harmful acoustic wave reflections at the transition to the port. Intake runner lengths were then chosen based on Helmholtz resonance calculations and experimentation in Ricardo Wave in order to target an acoustic tuning peak to complement that of the exhaust system. In order to manufacture the complex geometry, we chose to 3-D print the intake using Ultem 1010 for strength and ability to withstand high temperatures. To ensure structural integrity of the plenum, FEA was performed using the materials weakest orientation in order to determine rib placement to cut weight and minimize plenum wall deflection.

Drivetrain

The final drive was selected to maximize power output based on the engine torque curve, as well as reduce the number of times the driver has to shift. Because the car doesn't have a paddle shifting system, shifting is a more complex operation, so shifting more will take the driver's concentration away from driving the car. We chose a limited slip differential in order to gain the benefits of both a solid axle and open differential. Our LSD is a clutch-type, which makes it simpler to maintain and also allows for finer adjustability based on driver feedback and weather conditions. We chose to use an eccentric differential mounting system despite it being heavier than turnbuckles, as it provides consistent and reliable chain tensioning while preventing the diff from moving off axis.

Using free body diagrams, we developed a code to determine the force profile on the each tooth of the sprocket at different locations of the roller, which we used as boundary conditions for topology optimization. We validated our simulations through destructive testing via a pneumatic piston set up to imitate the loading the sprocket sees during use.

Cooling System

The cooling system was designed using a genetic algorithm, which minimizes the mass of the radiator given the engine operating temperature, ambient temperature, coolant flow rate, vehicle speed, target heat rejection, and geometric constraints. The average maximum heat rejection was determined by measuring the flow rate and temperature difference across the engine. Ambient temperature was determined from data available through the national weather service. Engine operating



temperature is specified in the engine service manual. Average vehicle speed was taken from Heat transfer in the radiator was calculated using pipe flow analysis, and effectiveness was calculated using the ϵ -NTU method. The radiator was mounted at an angle to minimize its front facing area and reduce drag. Windtunnel testing was conducted to ensure that angling the radiator did not result in a loss of effectiveness.

Electronics

Harness-

We established a goal for the 2019 season to reduce wiring harness weight as much as possible while maintaining durability and reliability. Electrical components were placed so as to minimize wire length for weight savings. This new placement requires that some components be moved closer to exhaust headers, but validation shows that all components remain within safe operating temperature. The maximum current and voltage ratings for every connection on the car was researched, which allowed us to select the minimum safe wire gauge for each connection. Wires which carry large amounts of current or differential signals run in twisted pairs. Bundles running to and from the same components are twisted, and all wires are color coded by function for organization.

Driver Interface-

Our goal was to make the information and buttons on the dashboard as accessible and intuitive as possible. To maximize readability, the numeric display was chosen to maximize digit size and brightness. While the shift lights above the numeric display always indicate engine RPM, the driver can toggle the numeric display between engine RPM and vehicle speed via buttons placed near the driver's thumbs. To facilitate quick interpretation of the display value, the first two of four numbers turn completely off when speed is being displayed so the driver can easily tell which display mode is activated. During testing, these buttons can be used to toggle between additional sensor values from the CAN bus.

Data Acquisition-

An important quality in a data acquisition system is modularity. To that end, we designed a PCB which interfaces with the car's various sensors and relays the information to a CAN bus. This design allows us to attach an arbitrary number of sensors and sensor boards, and therefore provides a highly modular data acquisition system. An additional "data logger" PCB saves all CAN Bus data locally to a Micro SD card, and broadcasts the data over radio. Select data is not broadcast in real time due to bandwidth limitations, but can be transmitted after the car is finished running. The transmitted data is both logged and displayed in real-time by a web-based application. This approach allows team members to both monitor the car's performance while running, and validate designs with in-depth data later. Our radio was chosen for its range and relatively high data rate. The chip that runs all of our PCBs was chosen for its speed, built in CAN controller, and ease of programming.

Cockpit, Controls, and Ergonomics

Braking-

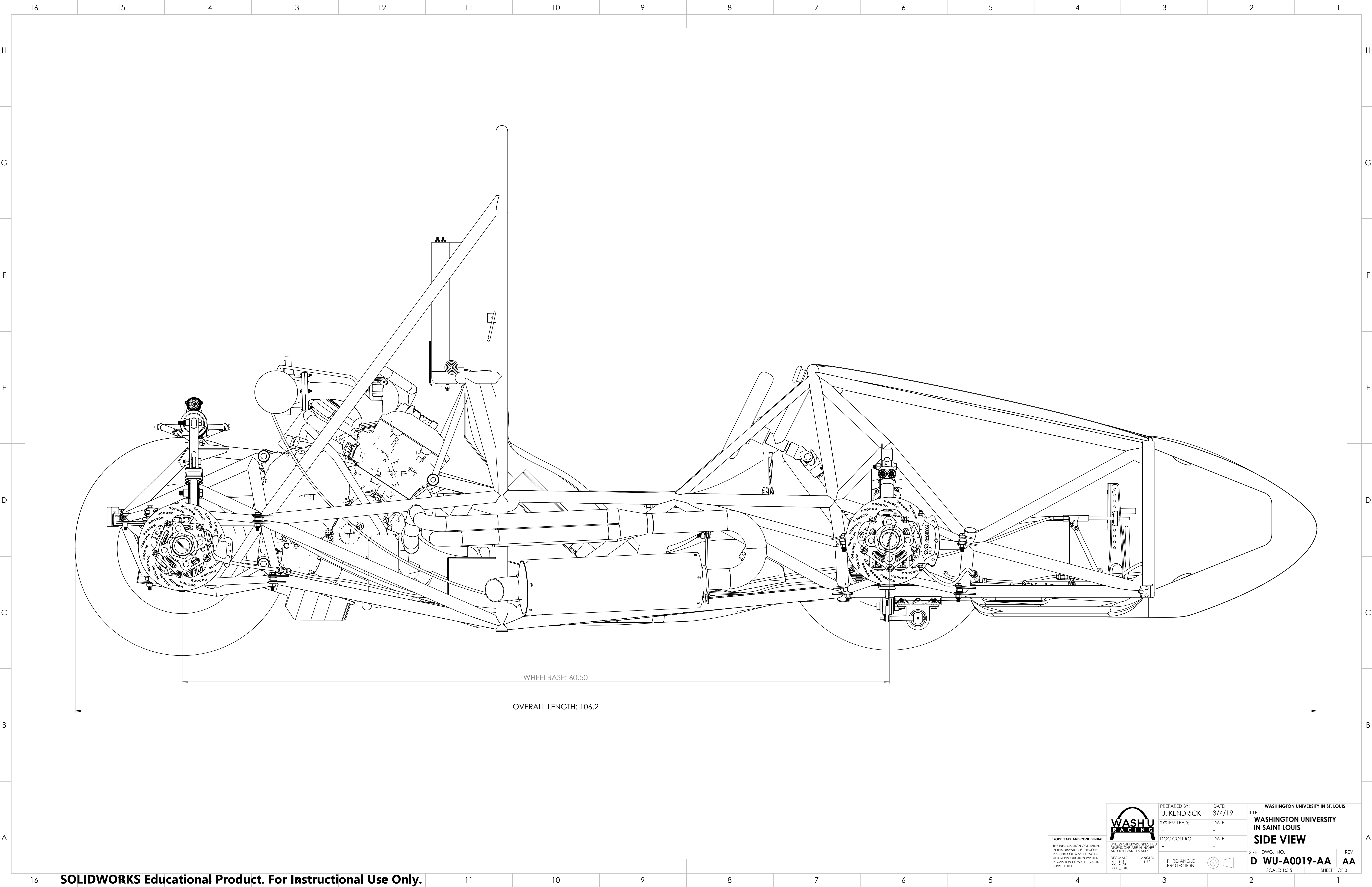
The brake system design started as a series of moment and force balance equations that were then used to find the required brake torque for the car. We chose our brake rotor material due to its low coefficient of thermal expansion. The rotor diameters were decreased to accommodate our wheel size, but kept as large as possible for maximum torque. System weight was reduced by using malleable copper hard lines rather than braided steel flexible brake lines. These copper lines allowed for a much more forgiving construction of the brake line network, as well as allow for use of more reliable fittings to reduce potential of leaking brake lines that could then lead to brake pressure loss. Brake line pressure sensors allow us to monitor our pressure to see if our bias needs adjusting.

Seat-

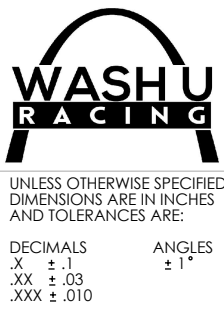
In order to maximize driver comfort and support while the car is in motion, the seat was contoured to a RAMSIS manikin, which is a dynamic, humanoid 3D model that can be positioned within CAD models. This particular manikin was produced by inputting the anthropometric data of several of our drivers into RAMSIS. The result of this contouring is a snug fit around the driver's body, which will ultimately aid in reducing driver fatigue because they will not have to expend as much energy keeping their torso rigid while cornering. The seat has a rigid carbon fiber construction.

Pedals-

The design of the pedal box was focused primarily on being easily adjustable. The entire pedal box sits on a rack that has 12 adjustable positions over 4 inches and can be adjusted with one hand. A combination of carbon fiber and aluminum components were used to both keep weight at a minimum and reduce compliance in the system. To verify this, destructive testing was done on our brake pedal to identify points of failure and validate the accuracy of our FEA.



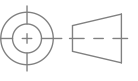
PROPRIETARY AND CONFIDENTIAL
THE INFORMATION CONTAINED
IN THIS DRAWING IS THE SOLE
PROPERTY OF WASHU RACING.
ANY REPRODUCTION WITHOUT
PERMISSION OF WASHU RACING
IS PROHIBITED.



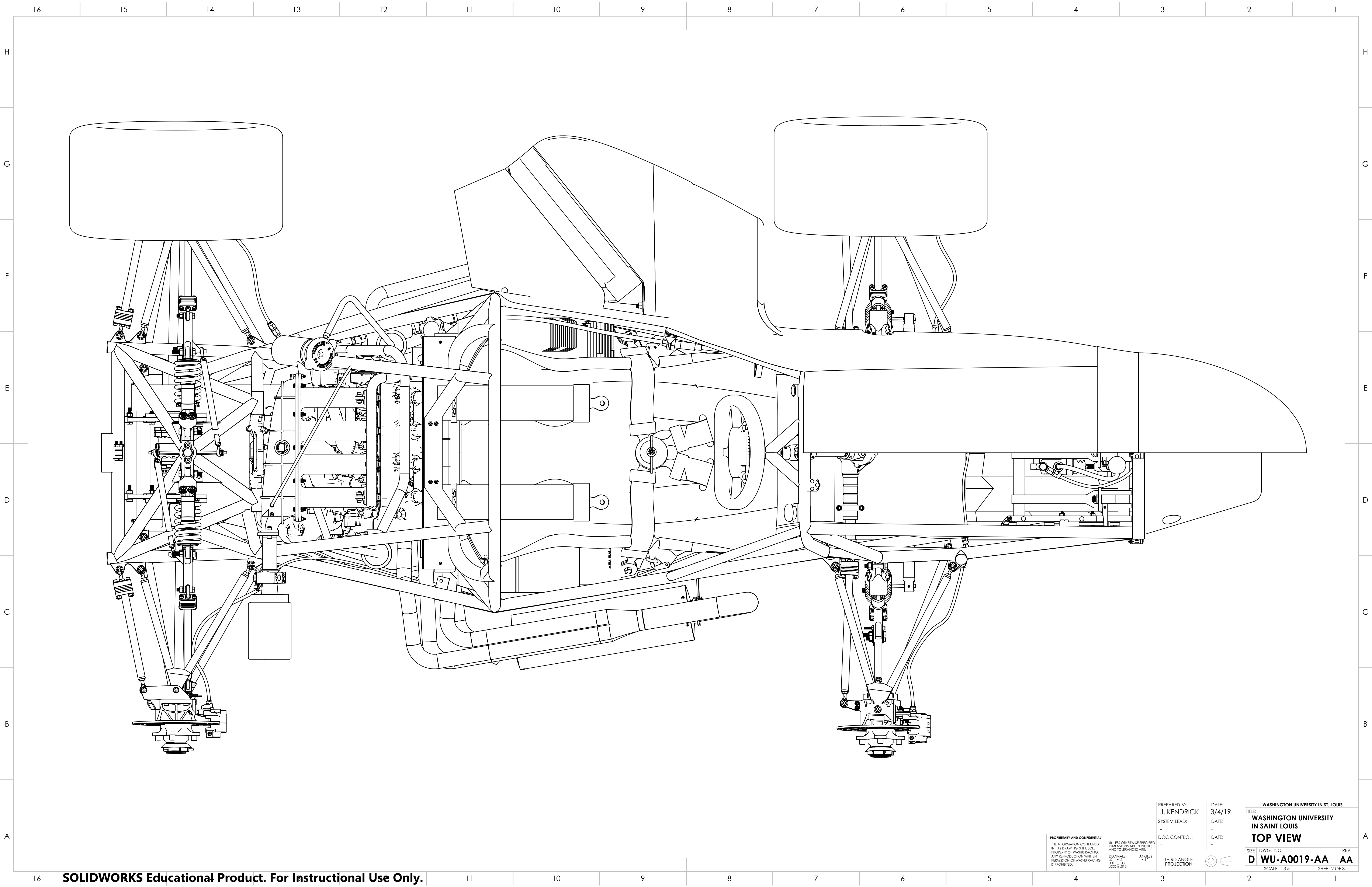
PREPARED BY:
J. KENDRICK
SYSTEM LEAD:
-
DOC CONTROL:
-

DATE:
3/4/19
DATE:
-
DATE:
-

THIRD ANGLE
PROJECTION



WASHINGTON UNIVERSITY IN ST. LOUIS
TITLE:
WASHINGTON UNIVERSITY
IN SAINT LOUIS
SIDE VIEW
SIZE DWG. NO.
D WU-A0019-AA
SCALE: 1:3.5
REV
AA
SHEET 1 OF 3



PROPRIETARY AND CONFIDENTIAL
THE INFORMATION CONTAINED
IN THIS DRAWING IS THE SOLE
PROPERTY OF WASHU RACING.
ANY REPRODUCTION WITHOUT
PERMISSION OF WASHU RACING
IS PROHIBITED.

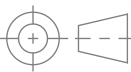
UNLESS OTHERWISE SPECIFIED
DIMENSIONS ARE IN INCHES
AND TOLERANCES ARE:
DECIMALS
X - ± .03
XXX ± .010

ANGLES
± 1°

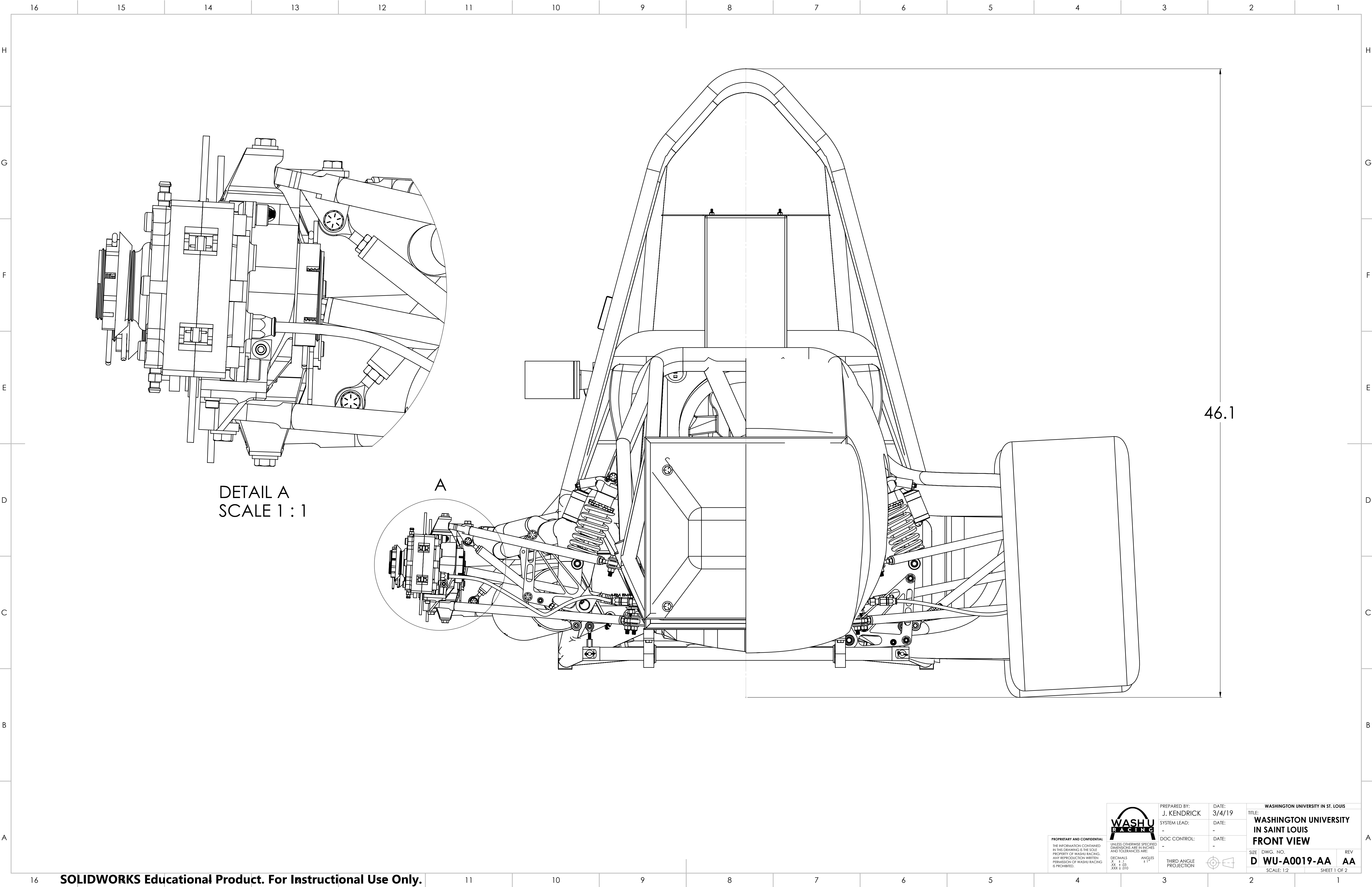
PREPARED BY:
J. KENDRICK
SYSTEM LEAD:
-
DOC CONTROL:
-

DATE:
3/4/19
DATE:
-
DATE:
-

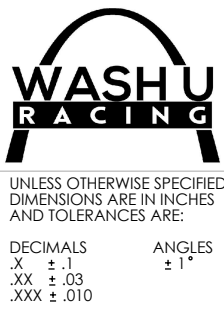
THIRD ANGLE
PROJECTION



WASHINGTON UNIVERSITY IN ST. LOUIS
TITLE:
WASHINGTON UNIVERSITY
IN SAINT LOUIS
TOP VIEW
SIZE DWG. NO.
D WU-A0019-AA
SCALE: 1:3.5
REV
AA
SHEET 2 OF 3



PROPRIETARY AND CONFIDENTIAL
THE INFORMATION CONTAINED
IN THIS DRAWING IS THE SOLE
PROPERTY OF WASHU RACING.
ANY REPRODUCTION WITHOUT
PERMISSION OF WASHU RACING
IS PROHIBITED.

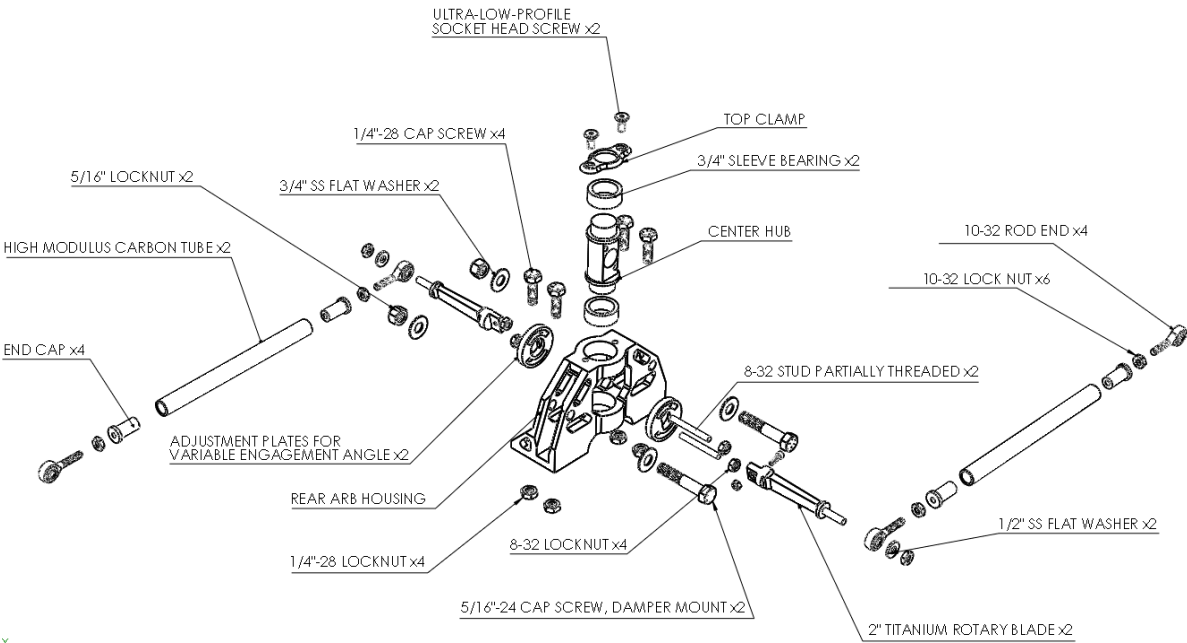


PREPARED BY:
J. KENDRICK
SYSTEM LEAD:
-
DOC CONTROL:
-
THIRD ANGLE
PROJECTION

DATE:
3/4/19
DATE:
-
DATE:
-
THIRD ANGLE
PROJECTION

WASHINGTON UNIVERSITY IN ST. LOUIS
TITLE:
WASHINGTON UNIVERSITY
IN SAINT LOUIS
FRONT VIEW
SIZE DWG. NO.
D WU-A0019-AA
SCALE: 1:2
REV
AA
SHEET 1 OF 2

Exploded view of WUFR-19 Rear ARB Assembly with adjustable rotary blades



Exploded View of WUFR-19 Adjustable Peddle Box

